

Supplemental Data S1: interpretation of diffraction patterns

This section presents the basic equations underlying the interpretation of the diffraction patterns of the (200) and (004) crystal planes of cellulose. A diffraction pattern results from the contributions of all cellulose crystallites in the wood piece crossed by the X-Ray beam. Both the fact that a given crystallite contributes or not and the position of the diffracted spot depend on the orientation of the crystallite. In this set-up, the beam passes wood perpendicular to the fibre axis, so that the orientation of the microfibril axis can be specified by two angles: the microfibril angle μ , and the local orientation of the wall α (Fig. S1). For each crystal plane, (200) or (004), the diffraction occurs when the angle between the incident beam and the crystal plane is equal to the Bragg angle θ_{200} or θ_{004} .

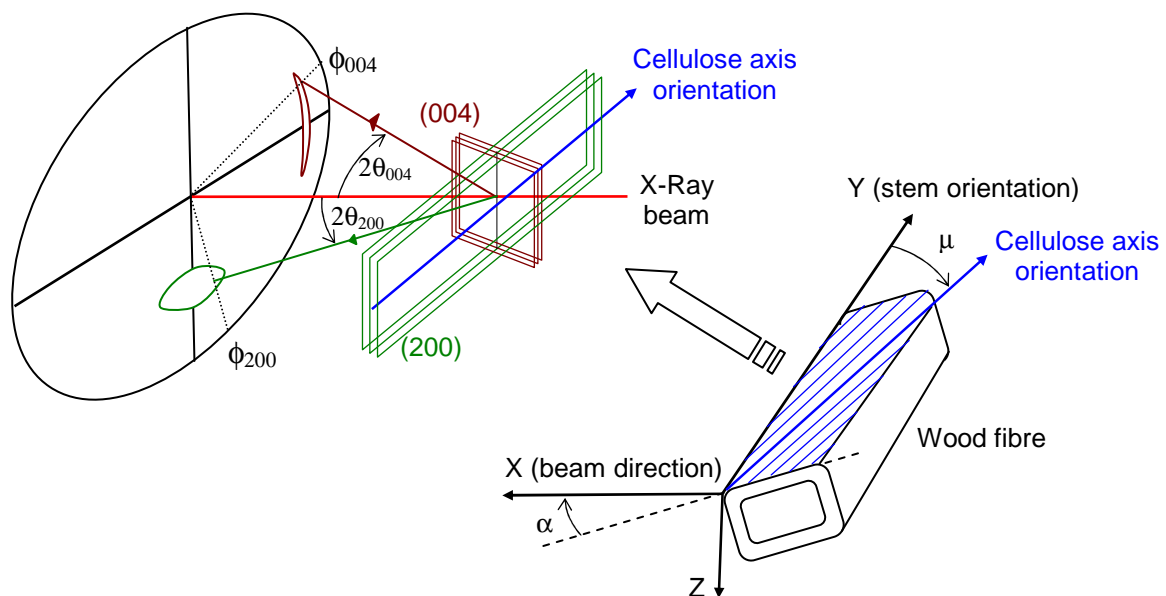


Figure S1. Schematic representation of the contribution to diffraction of a given microfibril of the wood fibre. μ : microfibril angle; α : orientation of the wall containing the microfibril; θ : Bragg angle; ϕ : azimuth on the screen of the contribution to the diffraction pattern.

Diffraction of the (004) crystal plane

The condition for diffraction of the (004) plane can be expressed as:

$$\sin\mu = \sin\theta_{004}/\cos\alpha \quad (1)$$

For each wall orientation α , there is at most one microfibril angle μ that satisfies equation (1) and therefore contributes to the diffraction. In case of diffraction, the beam is deviated at an azimuth angle ϕ_{004} given by:

$$\tan\phi_{004} = \sin\alpha*\tan\mu \quad (2)$$

Solving equations (1) and (2), each azimuth of diffraction ϕ_{004} can be associated to a single value of microfibril angle μ (Fig. S2).

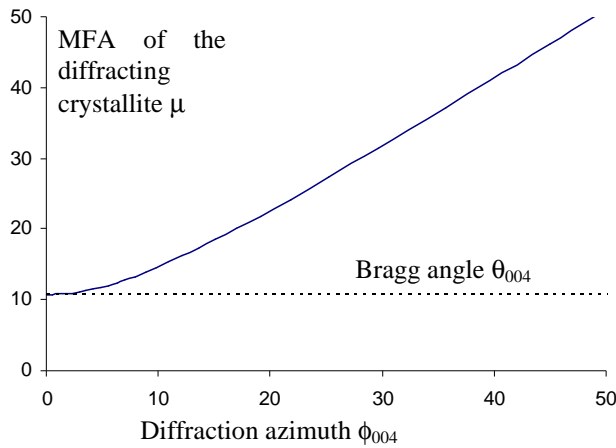


Figure S2. Relation between the azimuth of the contribution to (004) diffraction and the microfibril angle of the contributing crystallite (for a beam passing perpendicular to the stem).

Diffraction of the (200) crystal plane

Cave (1997) solved the problem for the (200) crystal plane. Assuming that the rotation angle of the (200) plane relative to the microfibril axis is random and uniform, he showed that the condition for diffraction resumes to:

$$\tan\theta_{200}.\cos\alpha + \sin\alpha.\cos\phi_{200} + \cot\mu.\sin\phi_{200} = 0 \quad (3)$$

If walls were all oriented perpendicular to the beam ($\alpha=\pi/2$), equation (3) would simply become $\phi_{200}=\mu$ (or $\mu+180^\circ$), so that the diffraction pattern would be the direct image of the MFA distribution. In the general case, various combinations of (α,μ) can diffract at the same azimuth, so that the diffraction at a given azimuth cannot be associated to a single value of the MFA. However, the contribution of walls that are not perpendicular to the beam results in a

distortion of the diagram mainly at small azimuth angles, and the diffraction pattern can be interpreted to get information about the MFA distribution.

Numerical assessment of MFA distributions in cell wall layers

We developed a numerical model that computes the theoretical (200) diffraction pattern, for a given set of parameters describing the cell shape, the cell-wall layering, the cellulose content and MFA in each layer, and the variability of these parameters in the wood sample. We compared the outputs of this model to the measured diffraction patterns in order to assess our interpretations of MFA distribution. The fibres are assumed to have a rectangular shape with rounded corners (Fig. S3), and the cell walls are made of 3 layers with specific MFA distributions.

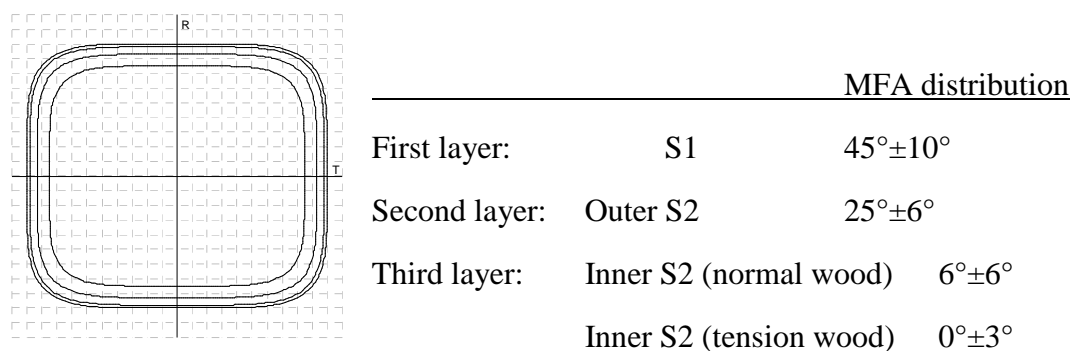


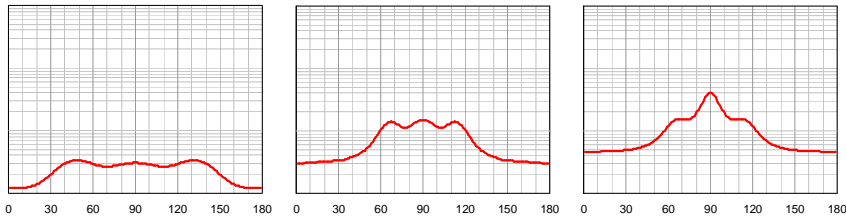
Figure S3. Wood fibre geometry and MFA distribution for the diffraction model

The distribution of wall orientations in a fibre was computed from this geometry. The distribution of wall orientations in the wood tissue was then computed accounting for the variability of fibres arrangement (random error of 3° for the fibre axis direction and 15° for the rotation of R and T walls). The 3-D distribution of microfibril orientation was then computed using the parameters of MFA distribution in each layer. The complete diffraction patterns are computed using equation (3) and the 3-D distribution of microfibril orientation, for different stages of cell wall formation. The chosen parameters of MFA distribution yield a good agreement between the simulated diffraction patterns and experimental results (compare Fig. S4 to Figs. 2-3 of the article).

Normal wood: A1

A2

A3 – A4



Tension wood: A1

A2

A3

A4

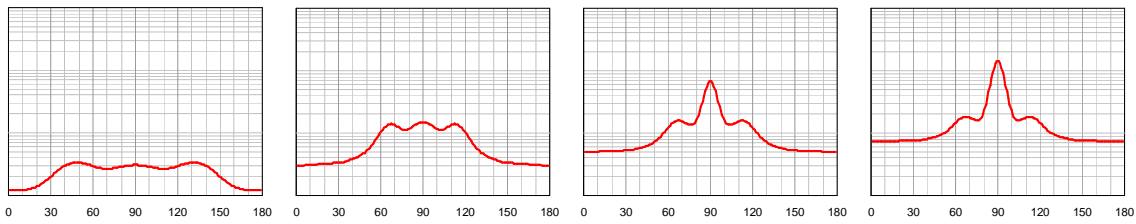


Figure S4. Simulated diffraction patterns with adjusted MFA distribution for tension and normal wood at different stages of development:

A1: S1 layer only

A2: S1 + outer S2 layer

A3: S1 + outer S2 + inner S2 layer (half thickness for tension wood)

A4: S1 + outer S2 + inner S2 layer (full thickness for tension wood)

Supplemental Data S2: changes in lattice spacing in all studied profiles

The evolution of lattice spacing along all studied sequences of wood development are shown in Fig. S5 (profiles shown in the results of the article are TW2a and NW1c). In tension wood stems, all profiles at small angles (except TW1a) show an increase of the d_{004} during the thickening of the layer. Profiles for large angles do not display a common trend. In TW1a, the low intensity of the signal made the detection of the peak value difficult resulting in a high dispersion of lattice spacing estimates. In the 5 other scans the dispersion is comparatively low and allows a clear observation of the change in lattice spacing along the sequence. The lattice strain (relative change in lattice spacing) ranges between 0.18% and 0.30%. In normal wood, d_{004} remains mainly constant along the sequence.

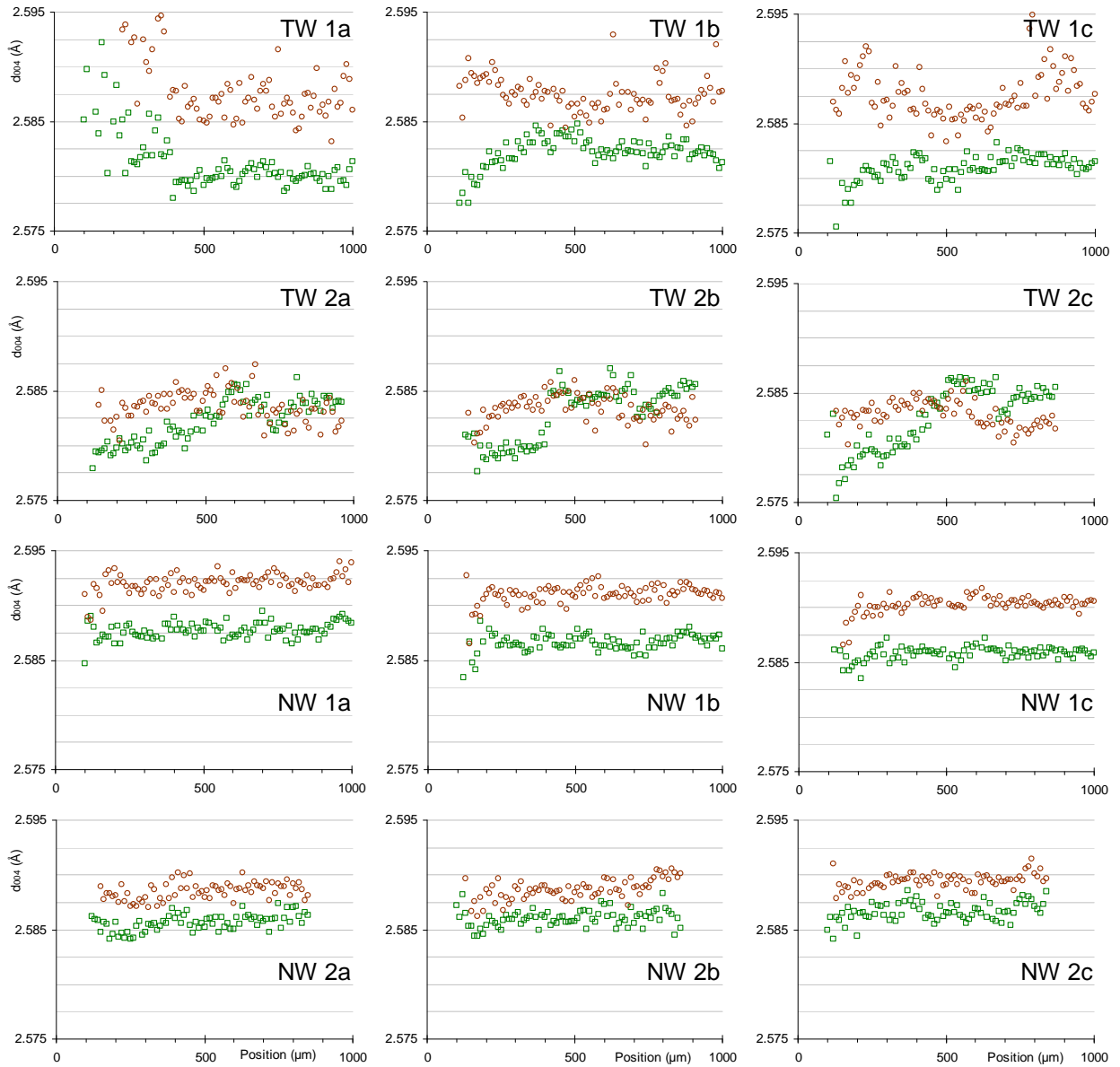


Fig. S5: Lattice spacing (d_{004}) along sequences of wood cell wall development, with distinction between the contributions of microfibrils oriented with large angle ($>16^\circ$, red circles) and small angle ($<16^\circ$, green squares). TW: tension wood, NW: normal wood. 1, 2: stem number. *a, b, c*: successive scans on the same stem at 3 different positions.